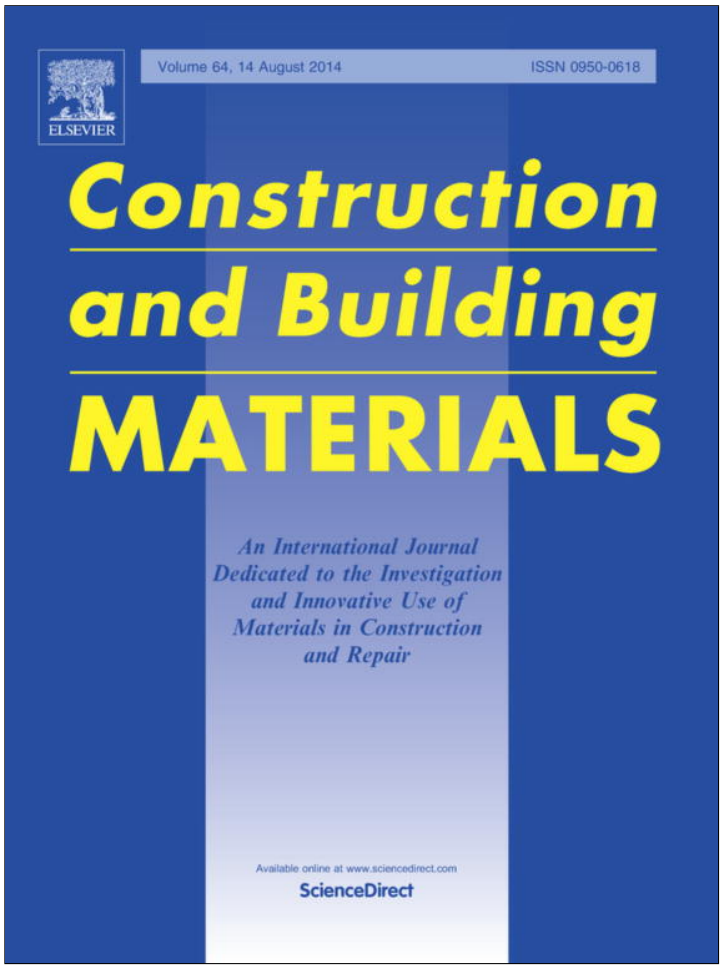

Construction and Building Materials 64 (2014) 431–439

Contents lists available at ScienceDirect

Construction and Building Materials

journal homepage: www.elsevier.com/locate/conbuildmat

Adhesive bonding of fire-resistive engineered cementitious composites (ECC) to steel

Qian Zhang, Victor C. Li *

Department of Civil and Environmental Engineering, University of Michigan, Ann Arbor, MI 48109-2125, USA

HIGHLIGHTS

- Acrylic latex improves the FR-ECC matrix/steel interfacial adhesion.
- The enhancement is attributed to a change in ITZ composition and microstructure.
- Acrylic latex admixture reduces the ductility of FR-ECC, however it can be restored.
- FR-ECC possesses notably enhanced mechanical and adhesive properties over SFRM.

ARTICLE INFO

Article history:
Received 22 January 2014
Received in revised form 19 March 2014
Accepted 4 April 2014
Available online 5 May 2014

Keywords:
Fire-resistive engineered cementitious composites
Adhesion
Latex
Steel
Durability
Tensile ductility

ABSTRACT

Recent research has demonstrated the feasibility of developing a fire-resistive engineered cementitious composite (FR-ECC) to address the current issue of lack of durability (adhesion and cohesion) of spray-applied fire-resistive materials (SFRM) on steel structures. FR-ECC was shown to possess inherently better cohesive properties over conventional SFRM, facilitated by its relatively high tensile strength and ductility. This paper aims at tailoring the FR-ECC for enhanced adhesion and characterizing its adhesive property to steel substrate. Specifically, an acrylic latex bonding agent was used as admixture in FR-ECC and as an interfacial adhesive, and a fracture mechanics based adhesion test method was adopted to quantify the change in adhesive property. Based on the measured adhesion between latex modified FR-ECC matrix and steel, using latex as admixture and interfacial adhesives effectively improved the interfacial adhesive energy of FR-ECC matrix by 54% and 147%, respectively, compared to unmodified one. Environmental scanning electron microscopy revealed changes in composition and microstructure of the interfacial transition zone (ITZ) between latex modified FR-ECC matrix and steel, which resulted in the higher adhesive bond. The effect of latex addition on the mechanical performance of FR-ECC was also studied and discussed in this paper.

1. Introduction

Engineered cementitious composite (ECC) has been developed over the last decade as an alternative infrastructure material to conventional concrete. ECC belongs to the family of high performance fiber reinforced cementitious composites designed for high tensile ductility and can flex instead of fracture under extreme bending load. Its uniaxial tensile strain capacity is 3–5%, about 300–500 times that of normal concrete. This characteristic distinguishes ECC from almost all kinds of concrete, fiber reinforced or not, that typically has tensile strain capacity on the order of 0.01% [1]. Originally developed for earthquake resistant structures, it has since been applied to full-scale building, transportation, water and energy infrastructures in Europe, Asia and the US for enhanced safety, durability and sustainability [2].

Recent study demonstrated the feasibility of using lightweight ECC as a passive fire-resistive material [3]. Fire-resistive ECC (FR-ECC), combining the thermal insulating property and high tensile strength and ductility, was developed to address the lack of durability issue with conventional spray-applied fire-resistive material (SFRM). The durability of the fire-resistive material is recognized to include two major aspects: cohesion and adhesion [4]. FR-ECC was shown to have inherently better cohesive property compared to conventional brittle SFRM, and therefore possesses enhanced durability [3].

Another important target performance of FR-ECC is strong adhesion to steel. Up to now, there has been no published information on the characterization of the adhesion of ECC material in general, and FR-ECC in particular, to steel. This research is intended to fill this knowledge gap.

* Corresponding author. Tel.: +1 734 764 3368.
E-mail address: vcli@umich.edu (V.C. Li).

http://dx.doi.org/10.1016/j.conbuildmat.2014.04.059
0950-0618/

The current SFRM/steel bond-testing standard is the so-called "mayonnaise cap" standard testing procedure [5], which is a strength-based test. This measurement approach does not differentiate between different failure mechanisms, nor does it measure the true material property since it is specimen-size dependent [6]. It also heavily relies on the operators' individual testing protocol and judgment. Recently, National Institute of Standard and Technology (NIST) developed a material science based approach using linear fracture mechanics principles to experimentally determine the adhesion between spray-applied fire-resistive materials (SFRM) and steel [6,7]. This fracture-based test method was proposed as an alternative to the strength-based standard test and proved to measure the true material properties in a more rigorous manner. Enhancing the adhesion and proper characterization of the adhesive bond between FR-ECC and steel are necessary to fully evaluate the performance and potential of FR-ECC before large-scale testing and field applications.

Previous researches [8–14] have shown that polymer latex addition is effective in strengthening the interfacial bond between cementitious material and various types of substrate including steel. The improvement is associated with the enhancement of interfacial transition zone between cementitious material and other surfaces [13,15–17]. Studies also demonstrated that for low volume content of latex addition, the non-combustible nature of the latex modified cementitious composites remained unchanged [16,18] making it suitable for FR-ECC application. In this study, commercially available acrylic polymer latex was adopted as admixtures and interfacial adhesives to modify the FR-ECC/steel bond. It is hypothesized that the utilization of polymer latex will lead to enhanced adhesion properties of FR-ECC to steel.

The inclusion of polymer admixtures into ECC may result in a change in the microstructure and micromechanical properties of ECC that may alter its mechanical properties. According to ECC design theory, the macroscopic mechanical property (tensile strength, tensile ductility, crack widths, etc.) can be linked to the microscopic microstructural and micromechanical properties (matrix toughness, flaw size and distribution, fiber geometry, fiber mechanical properties, fiber/matrix interfacial bond properties, etc.) [19–21]. Ohama found that when latex is mixed with cementitious material, a polymer film envelops the cement hydrates and aggregate surface due to coalescence of polymer particles and therefore a cement–polymer co-matrix is formed in such material. In ordinary concrete materials, the cement hydrates (C–S–H and C–H) are considered to be bound together by weak van de Waals force, resulting in low fracture toughness and tensile strength [22]. The formation of a co-matrix in latex-modified cementitious material provides a stronger bond between cement hydrates, and between paste and aggregates, thereby improving the fracture toughness and tensile strength of such material [23–26]. Also, the bond between matrix and polymer fibers may be expected to be stronger in latex modified fiber-reinforced composites. In addition, increased air entrainment with polymer addition has been observed [22,24]. These changes in matrix properties and fiber/matrix interfacial bond could lead to competing effects on the tensile performance of ECC, according to micromechanical models. No research has been performed on characterizing the impact(s) of latex admixtures on the tensile and compressive mechanical performance of ECC, and FR-ECC in particular.

In this study, the effectiveness of employing polymer latex bonding agent as admixtures and interfacial adhesives was evaluated using a recently developed fracture-based adhesion test method. Microscopic investigation was conducted to study the mechanisms of the adhesion enhancement. In addition, the impact of polymer modification on the mechanical behavior of FR-ECC was assessed by direct uniaxial compression and tension test. Experimental results and findings are documented in this paper.

2. Experimental programs

2.1. Material

The previously studied FR-ECC mixture [3] is listed in Table 1 (Mix 1). Acrylic latex-based bonding agent was adopted as admixture in Mix 2 and 3. The solid latex/cement weight ratio of Mix 2 and 3 were 1.875% and 3.75% respectively. The latex was added as a replacement of water as recommended by the manufacturer, thus avoiding increasing water/cement ratio. Mix 4 was identical to Mix 1 except that the bonding agent was applied directly on the steel/FR-ECC interface to facilitate adhesion. Type I ordinary Portland cement (OPC) conforming to the requirements of ASTM C150 was used in all Mix 1–4. Polycarboxylate-based high range water reducing (HRWR) admixture and viscosity modifying agent (VMA) were used simultaneously to obtain proper workability and control of fiber dispersion. Micro-spherical glass bubbles and PVA fibers were used in all mixtures. The characteristics of glass bubbles and PVA fibers are listed in Tables 2 and 3, respectively. The addition of glass bubbles is intended to attain thermal properties for insulation purpose [3]. In the adhesion characterization study, 0.5% fibers (by volume fraction) were used for Mix 1–4, which will be further explained in Section 2.2. In the study on mechanical properties of FR-ECC, 2% fibers (by volume fraction) were used for Mix 1–3. Specimens of one type of commercially available Portland cement-based medium density SFRMs were also prepared in accordance with manufacturer's guide as control specimens for comparison purposes.

2.2. Adhesion characterization

To properly characterize the adhesion between the previously described mixtures and steel substrate, a linear elastic fracture mechanics based method [6,7] was adopted in this research. This approach measures the fracture energy G_c to characterize the adhesion of the SFRM/steel assembly in "peeling" mode. The experimental configuration is illustrated in Fig. 1. It involves peeling a thin steel strip off the slab composed of the fire-resistive material. The load, displacement and crack length are recorded during the test. This configuration is modeled as lifting of an elastic beam on a flexible foundation; the critical energy release rate G_c can be calculated as [6]

$$G_c = \frac{6P^2(\lambda a + 1)^2}{E_{steel} b^2 \lambda^2 h_{steel}^3} \tag{1}$$

where P is the load in equilibrium with the extended crack length a; E_{steel} is the elastic modulus of steel; b and h_{steel} are the width and thickness of the steel strip respectively; λ is a coefficient associated with the stiffness of the foundation and can be calculated as [6]:

$$\lambda = \left(\frac{3E_{SFRM}}{E_{steel} h_{SFRM} h_{steel}^3}\right)^{\frac{1}{4}} \tag{2}$$

where E_{SFRM} is the elastic modulus of the SFRM (or Mix 1–4) and h_{SFEM} is the thickness of the SFRM (or Mix 1–4) slab. Eq. (1) is valid for the case of sufficient bonded length between steel and the slab (greater than 25 mm in this configuration).

Eq. (1) (and the fact that $G = G_c$ during crack propagation) leads to $\frac{dG}{da} > 0$ implying unstable crack growth. However, under displacement control test, the load will drop as the crack extends, resulting in crack arrest. As a result, multiple pairs of P–a can be measured in a single specimen.

The specimen was prepared by placing the steel strips at the bottom of the mold and casting the fire-resistive material to form a specimen as shown in Fig. 2. Structural steel strips of 12.7 mm wide and 1.27 mm thick were placed at a center-to-center space of 50 mm. The thickness of casted material (Mix 1–4 and control SFRM) was approximately 25 mm. The steel surface was roughened using sanding paper and cleaned with alcohol, and then a pre-crack of 12.7 mm was formed by applying nonstick Teflon tape at one end of the steel strip. Mix 1–4 with 0.5% volume fraction of fibers were used to prepare the adhesion specimen. Adhesion tests were conducted at 14 days after curing the specimens at laboratory room condition (23 ± 3°; 30 ± 10% RH).

This study focuses on the effect of the admixtures and surface adhesives on the adhesion, which is assumed to be mostly associated with the matrix property. A minimum fiber content (0.5%) was used to avoid large measurement deviation caused by inhomogeneity of the material associated with fibers. The small amount of fiber was included to prevent premature fracture of the FR-ECC matrix panel due to gripping during testing. As reported in Section 3.3, a re-test of G_c using an FR-ECC with 2% fiber shows similar results as for these specimens with lower fiber content.

The experiment was conducted on an electrodynamic load-frame with an attached S-beam load cell for higher precision (0.04 N accuracy). During the test, the steel strip was lifted at one end (where the pre-crack was located) under a constant displacement rate of 1 mm/min. When crack extension occurred on the interface, correspondingly, there would be a load drop. The reduced load P was recorded. At this time, the test was aborted manually and the extended crack length 'a' was measured using a length scale with precision of 1 mm. Then the specimen was unloaded and reloaded until another crack propagation occurred. The complete

Table 1
Mix proportion (by weight) of the adhesion test specimen.

	Description	Cement	Water	Glass bubble	Bonding agent
Mix 1	FR-ECC [3]	1	0.75	0.5	0
Mix 2	Mix 1 with latex bonding agent as admixture	1	0.675	0.5	0.075
Mix 3	Mix 1 with latex bonding agent as admixture	1	0.6	0.5	0.15
Mix 4	Mix 1 with latex bonding agent applied on steel surface	1	0.75	0.5	NA

Table 2
Physical properties of glass bubbles.

Density, kg/m^3	380
Composition	Soda-lime-borosilicate glass
Average diameter, μm	40
Effective maximum diameter, μm	85
Isostatic crush strength, MPa	27.6
Softening point, °C	600

Table 3
Characteristics of PVA fibers.

Nominal strength, MPa	1620
Apparent strength, MPa	1092
Diameter, μm	39
Length, mm	8
Young's modulus, GPa	42.8
Elongation, %	6.0
Density, kg/m^3	1300

unloading of the steel strip was used to confirm that no plastic yielding occurred within the steel. For the same mix proportion, at least 4 steel strip specimens were tested.

Eq. (1) is a simplified equation; this equation no longer holds when the crack tip approaches the other end of the strip. Depending on specimens, typically 3–6 loadings were performed on the same specimen before the crack tip became too close to the other end of the steel strip.

2.3. Microstructure investigation

SEM images were taken from the fractured surfaces adjacent to the steel/cementitious material interface from the cementitious material side. Environmental Scanning Electronic Microscope (ESEM) facilitated by EDAX was used in this study and images were taken after the adhesion test without any polishing or grinding preparation of the specimen. These investigations allow the examination of the modes of failure at or near the fire-resistive material/steel interface, the microstructural makeup, and the chemical composition of the surface material exposed by the fracture surface of the various mixes.

2.4. Mechanical property

To further understand the effect of the latex addition on the mechanical property of FR-ECC, mechanical properties characterization of Mix 1, 2 and 3 (with 2% fiber content) was performed.

Compressive strength of the mixes was measured using a set of three cube specimens of side 50.8 mm. The test was conducted using a compression test system at a loading rate of 1300 ± 300 N/s in accordance with ASTM C109 [27].

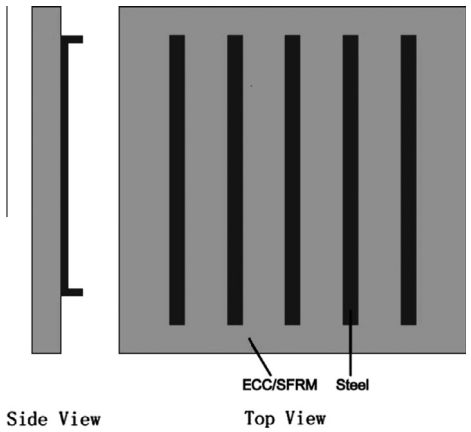

Fig. 2. Molding of multiple fire-resistive material/steel specimens.

Direct tension tests were conducted using the uniaxial tension test setup on a set of three specimens in accordance to Recommendations for Direct Tension Testing of High Performance Fiber Reinforced Cementitious Composites by the Japan Society of Civil Engineers [28]. A set of 3 dog-bone shape specimens were tested on a test system with 20 kN capacity, under a displacement control at the rate of 0.5 mm/min. Two external linear variable differential transducers (LVDTs) were attached to the specimen edges, with a gage length of approximately 101.6 mm, to measure the tensile strain.

All specimens were tested at the age of 28 days after curing under laboratory room conditions (23 ± 3 °C; 30 ± 10% RH). The compressive strength and tensile stress–strain curves of the mixes were obtained using the aforementioned test setups.

3. Results and discussion

3.1. Adhesion characterization

The G_c on the interface between the mixes and steel can be calculated at various crack length using Eq. (1). A typical G_c vs. crack length curve for FR-ECC (Mix 1) specimen is plotted in Fig. 3(a). As Fig. 3(a) shows, the curve reaches a plateau value. This indicates that small scale yielding behavior dominates. At smaller length (usually during the first loading), the measured G_c might be higher or lower than the plateau value. A plausible reason is that the crack initiates from the blunt pre-crack resulting in a G_c higher than the

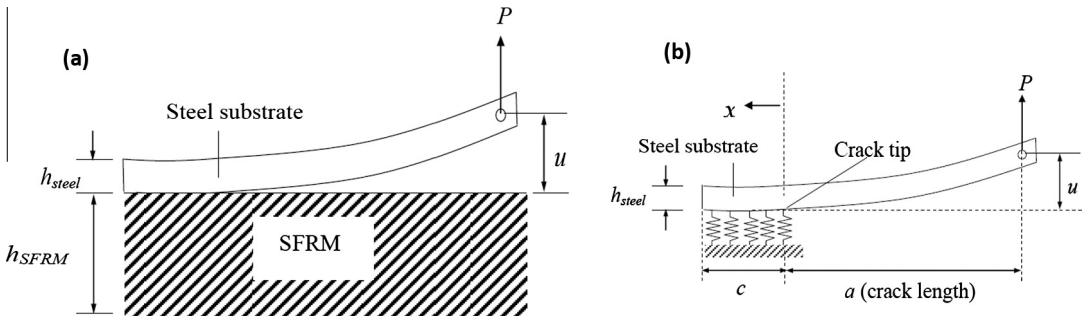

Fig. 1. Adhesion test [7] (a) specimen and load configuration, and (b) interface fracture model.

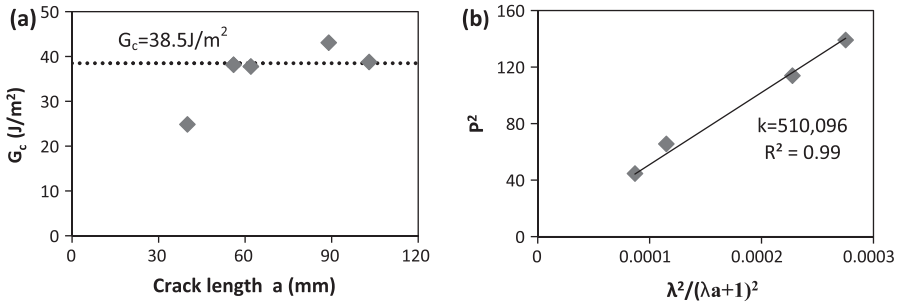

Fig. 3. Example of the data analysis of an adhesion specimen of Mix 1 (a) point-based calculation of adhesion energy on the specimen; (b) extraction of the adhesion energy from the slope of the curves.

plateau value, and this is often observed in control SFRM specimen. However, for Mix 1–4, the initial G_c values at small crack length may be below the plateau value, suggesting the possibility of a process zone development before small scale yielding becomes valid at larger crack length. The plateau value represents the steady-state critical energy release rate and is used to quantify the adhesion on the interface.

Due to the naturally large standard deviation with adhesion data, a further step of interpreting the data is taken to better extract useful information from the data. Using Eq. (1), P^2 can be plotted against $\frac{\lambda^2}{(\lambda a+1)^2}$ based on the data from the plateau regime, and linear regression of the data is then used to obtain G_c from the slope k of the best fit line. As shown in Fig. 3(b), linear regression is carried out on data derived from the Fig. 3(a), the coefficients of linear regression of most specimen are greater than 0.95. Then the adhesion energy is calculated as:

$$G_c = \frac{6k}{E_{steel} b^2 h_{steel}^3} \tag{3}$$

where E_{steel} is the elastic modulus of steel; and b and h_{steel} are the width and thickness of the steel strip, respectively. The mean value and standard deviation of the adhesion energy based on multiple specimens are then calculated. The results of G_c for all material tested are summarized in Fig. 4.

The adhesion test result shows that Mix 1 has a better adhesion to steel substrate than the SFRM control specimens and the adhesion is further improved by modifying the mixture with acrylic latex emulsion. The measured adhesion energy for SFRM is 11.1 J/m^2, this value is on the higher end of the reported data in the literature [6] for SFRM adhered to structural steel substrate (3–12 J/m^2). The control SFRM used in this study is a medium density, Portland cement-based SFRM reinforced with cellulose fiber, which could lead to a relatively higher G_c. Mix 1–4 all exhibit significantly higher adhesion than the control SFRM. Mix 2 performs significantly better (54% improvement) compared to unmodified Mix 1, which demonstrates that the addition of latex bonding agent as admixtures is effective in improving the surface adhesive property between such mix and steel substrate. However, the Mix 3 specimens do not have substantial improvement over unmodified Mix 1 specimen. It is suspected that excessive amount of water replacement by polymer latex can cause the paste to dry up too rapidly to allow sufficient time for the cementitious material to interact with the substrate at the interface. This observation is also consistent with previous research findings [12]. Consequently, Mix 3 will not be further investigated. Applying the bonding agent directly on the steel surface (Mix 4) is demonstrated to be the most effective method to improve the adhesion, which increases the critical energy release rate by 147% over that of Mix 1.

The failure mode of the FR-ECC (matrix) mixes is very different from that of the control SFRM. In SFRM specimens, crack propagation dominantly occurs within the cementitious material; while in FR-ECC specimens except for Mix 4, crack propagates at the interface between the cementitious material and steel. Fig. 5 shows the representative condition of steel strips peeled off from control

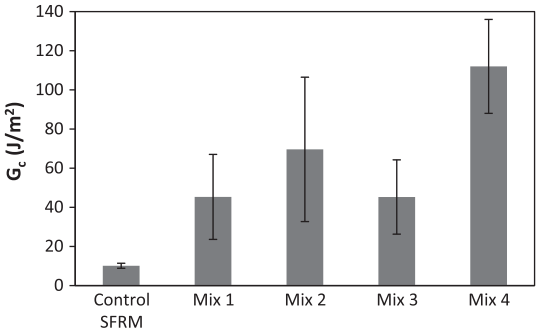

Fig. 4. The adhesion energy of FR-ECC matrices to steel is significantly higher than that of SFRM/steel.

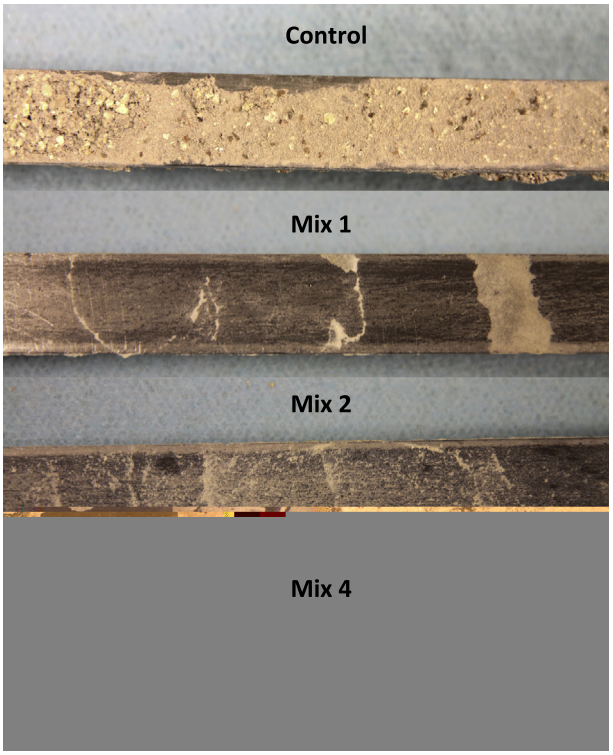

Fig. 5. The surface condition of peeled off steel strips from Mix 1, 2 and 4 is significantly different from that of control SFRM.

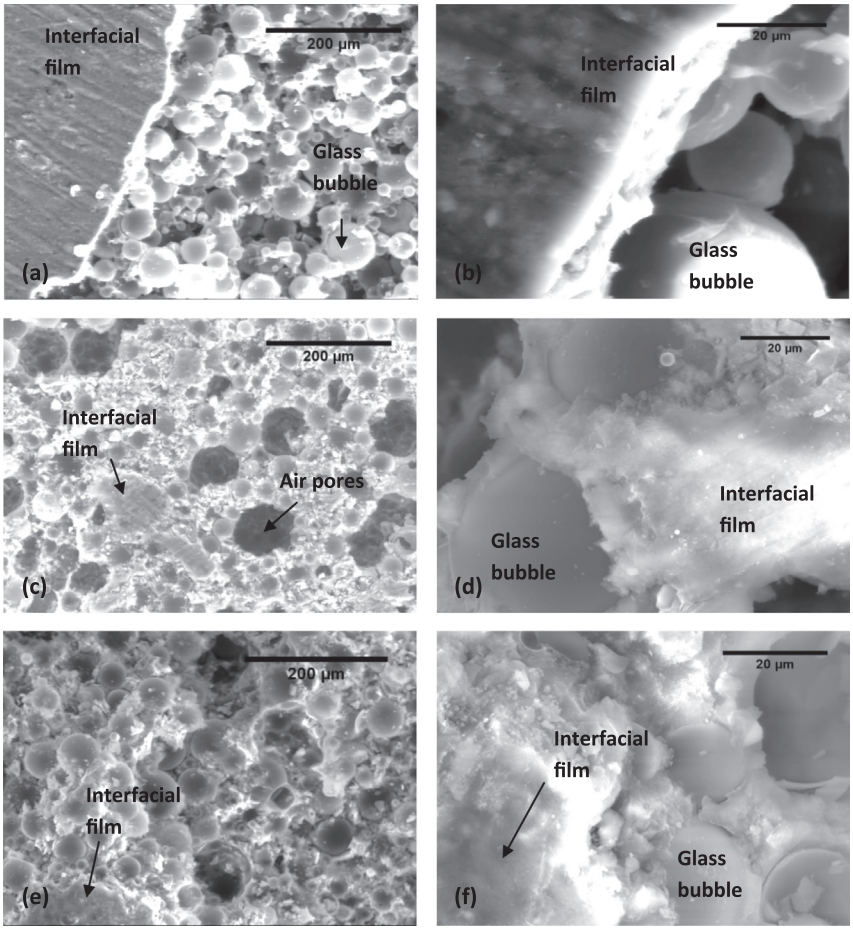

Fig. 6. SEM images of the interface (cementitious material side) of (a and b) Mix 1, (c and d) Mix 2, and (e and f) Mix 4.

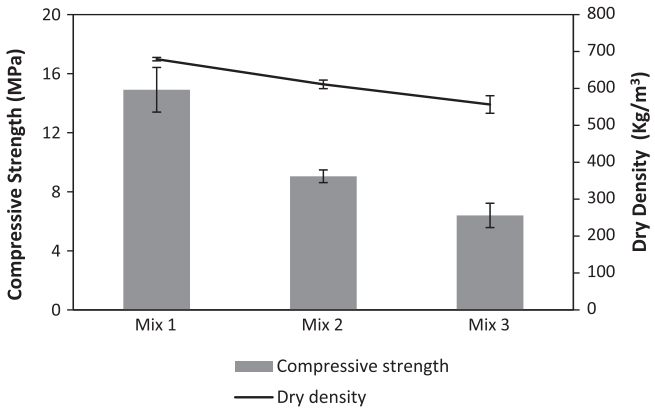

Fig. 7. Compressive strength and dry density of Mix 1, 2 and 3 decrease with increase in latex bonding agent dosage.

specimen, Mix 1, Mix 2 and Mix 4 after the adhesion test. It can be observed that for the control specimen, a relatively thick layer of cementitious material still adheres to the steel strip. For such material, the cohesive strength is very low; fracture failure within the SFRM material adjacent to the interface can be expected. In the case of Mix 1, apart from some spots, most of the area on the steel strip is clear of any cementitious residuals. This indicates that adhesive type of fracture occurs on the interface, which is quite different from the control specimen. Considering the fracture self-selects the plane requiring minimum energy for propagation, this adhesive fracture behavior reflects the influence of the higher cohesive (fracture toughness) property the FR-ECC (matrix) compare to the control SFRM specimen. For Mix 2, a very thin layer of cementitious film remains adhered to the steel substrate, which shows that the adhesive property has been improved in Mix 2 by the addition of latex polymer. However, this film is very thin and not continuous throughout the contact area. Mix 4 behaves very differently from Mix 1 and 2 specimens; a relatively thick layer of cementitious material adheres onto the steel strips through most of the contact area. This clear cohesive failure indicates a further improvement of adhesion on the interface. In addition, the much higher G_c suggests that the interfacial transition zone is also enhanced compared to Mix 2.

Failure on the interface is the dominant failure mode for FR-ECC (matrix) specimens, while cohesive failure is dominant in control SFRM specimens and Mix 4 specimen with bonding agent applied on steel surface. This also explains the larger variability in the test result of FR-ECC (matrix) specimens. Cohesion is an intrinsic material property while adhesion is an interfacial property, which is naturally subject to larger variability. It is demonstrated that higher interfacial bond as measured by G_c can be achieved (1) by enhancing the cohesive strength of the fire-resistive material (from SFRM to Mix 1), and (2) by enhancing the adhesive strength of the cohesively strong fire-resistive material/steel interface (from Mix 1 to Mix 2 and especially Mix 4).

3.2. Microstructure investigation

The micrographs of the interfaces from the cementitious material sides are presented in Fig. 6. The microstructure of the

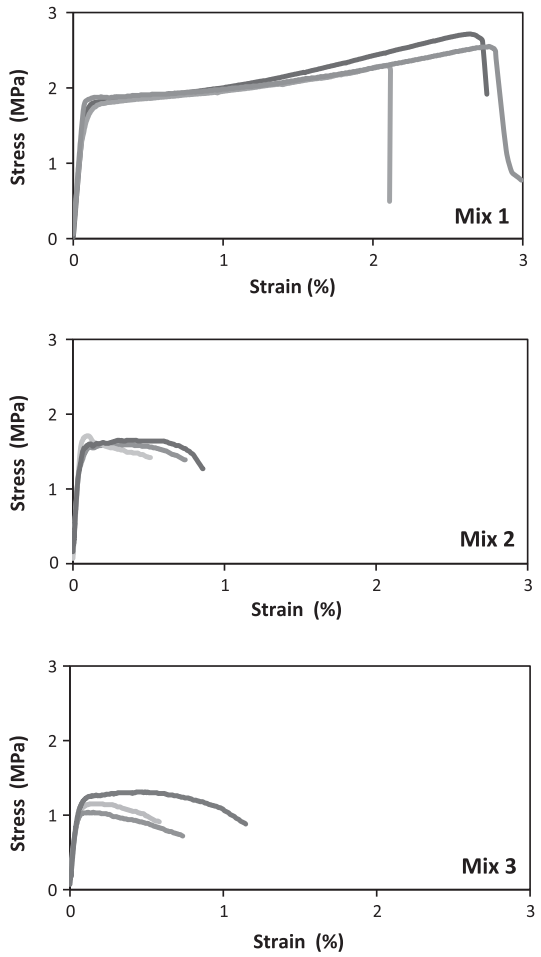

Fig. 8. Uniaxial tensile stress–strain curves of Mix 1, 2 and 3, showing the drastic reduction in tensile ductility with increase in bonding agent dosage.

interfacial part is a weak interfacial transition zone (ITZ) similar to that between cement paste and aggregate.

Fig. 6(a) shows a representative area of the interfacial layer of Mix 1 after the steel strip has been peeled off. On the left side of this image, a film formed right adjacent to the steel surface is visible, which covers most of the contact area of the specimen. It is a well-defined layer parallel to the steel surface even down to micron scale (Fig. 6(b)). This film is a solid layer of roughly ten microns thick. Below that solid film layer, the more porous matrix is formed with a large volume fraction of glass bubbles. EDAX analysis on the general area of the solid film reveals that the calcium to silica (C/S) ratio is around 3.0, which is much larger than the common C/S ratio of C–S–H (1.5–2.0 [29]). This indicates that it is a duplex film containing both C–S–H and C–H. Previous researchers [30,31] have also observed duplex films on the interface between cementitious material and other solid surfaces.

Fig. 6(c) shows the interfacial microstructure of Mix 2, which is Mix 1 modified by the addition of latex admixtures. From this figure, it can be observed that right adjacent to the interface, the solid layer was not continuous as in Mix 1 and most of the film has been peeled off during the adhesion test, leaving a much more porous material surface when compared to that of Mix 1. EDAX analysis shows the C/S ratio of the film is 1.93. This ratio lies within the C–S–H range indicating less (or no) C–H formation on the interface. A possible explanation for such change in the composition of the interfacial film can be found in the literature. The interfacial film is formed due to two effects: wall effect and bleeding, which result in a higher effective water to cement ratio, larger crystals of hydrated products and lower bond strength [30,32,33]. However, it has also been reported that the presence of polymeric materials (latex) alters the state of flocculation/coagulation and reduces bleeding [17] which can reduce the local effective water/cement ratio. In addition, the introduction of polymer chains increases the viscosity of the solution reducing ions mobility and dissolution [17,34]. These modifications of the ITZ by latex polymer favor the formation of C–S–H adjacent to the steel surface [35].

In addition, in Fig. 6(c), relatively large air pores with diameter up to 100 μm can be observed in the ITZ. The air pores are caused by the air entraining effect of latex emulsion during mixing. It can also be observed (Fig. 6(d)) that a polymer–cement co-matrix formed between glass bubbles. This is expected to enhance the bond between the cement paste and the glass bubbles, and therefore the fracture resistance. In contrast, glass bubbles are loosely packed in the matrix adjacent to the interface in Mix 1 as shown in the zoomed-in image (Fig. 6(b)).

Fig. 6(e) presents the microstructure of the interface of Mix 4/steel. The fracture surface moves further away from the interfacial film. The interfacial film is similar to that of Mix 2. Also, this film is densely bonded with glass bubbles (Fig. 6(f)) due to the high dosage of polymer bonding agent present on the interface. This enhancement extends to about 50 μm away from the surface due to the penetration of the bonding agent and results in a deeper and more tortuous fracture surface. The localized latex polymer also alters the film composition. As analyzed by EDAX, C/S ratio of this film is around 2.6, suggesting a duplex film with CH presence. This could be explained by the effect of polymeric material altering the flocculation and bleeding, together with the presence of high water content introduced by the latex emulsion.

The interfacial bond improvement with the use of latex admixture is associated with altering the interfacial layer composition and refinement of the porous ITZ. Further improvement can be expected by using anti-foaming agent along with latex admixtures to reduce the porosity of the mixture, especially in the ITZ. Applying the bonding agent directly on the surface alters the interfacial film composition, and enhanced the ITZ effectively without causing major air entraining effect. This is consistent with the highest adhesive bond G_c based on adhesive peel-off test reported in Section 3.1.

3.3. Mechanical property

The compressive strength and uniaxial tensile stress–strain curves for Mix 1, 2 and 3 are plotted in Figs. 7 and 8, respectively.

The compressive strength of the mixes under investigation decreases with increasing latex bonding agent dosage. This is mainly caused by the air entraining effect of latex bonding agent. The dry densities (measured at 28 days) of the mixes are also plotted in Fig. 7. It can be observed that the dry-density also decreases as the latex dosage increases, which indicates increased air content within the mixes. The dry density trend agrees well with the compressive strength decrease. Another possibility is that the viscosity increases significantly with the latex modification, which may cause difficulties in the processing and casting process, and this could contribute to the presence of larger flaws in the high latex content mixes. Thus, the benefit of latex addition on adhesive bond property is offset by a reduction in compressive strength. Nevertheless the compressive strength of Mix 1, 2 and 3 are all considered sufficient since fire resistive materials are considered nonstructural [36,37].

The tensile performance of FR-ECC is also affected by the latex admixture as shown in Fig. 8. The first crack strength drops from 1.78 MPa to 1.58 MPa and 1.10 MPa from Mix 1 to Mix 2 and Mix 3. The first crack strength is governed by the largest flaw size and the fracture toughness of the mix. The fracture toughness of

Fig. 9. Polystyrene beads used as artificial flaws.

the mix is expected to increase with latex addition, associated with the polymer–cement co-matrix formation. However, the air entraining effect of latex also causes larger flaws within the material, resulting in a competing effect. As the results show, the air entrainment effect appears to dominate, leading to the observed decreasing trend of first crack strength with latex addition.

The tensile ductility shows significant degradation with increased latex addition. From Fig. 8, we can observe that Mix 1 shows very consistent strain hardening with average strain capacity of 2.57%. Mix 2 shows inconsistent strain hardening behavior with significantly less strain capacity (<1%) and even softening behavior. Mix 3 shows consistent softening behavior featuring single crack opening. These phenomena might be associated with change in the interactions between matrix and fibers. The margin between the maximum fiber bridging stress σ_0 and the matrix crack strength σ_{cs} is critical to the tensile behavior. At stress level between σ_{cs} and σ_0, matrix cracks at multiple locations. The microcrack opening is the dominant component of the strain capacity. The more crack opens, the large tensile ductility the material exhibits. A higher σ_0/σ_{cs} often allows more crack openings and is associated with higher tensile ductility. As shown in Fig. 8, for Mix 2, the σ_0/σ_{cs} ratio is slightly higher than 1 in some specimens and below 1 in others. This lower margin is mainly attributed to a lower σ_0 value. One plausible reason for this lower σ_0 value is that the higher viscosity resulted from latex addition may have adversely affected the uniformity of the fiber dispersion and lead to lower fiber bridging capacity. Another plausible reason is a lower than intended fiber content due to the presence of air voids caused by the air entraining effect of latex admixtures; the 2% fiber content was calculated based on the rule of mixture without considering the air voids. The resulting lower σ_0/σ_{cs} could also explain the significant reduction in ductility from Mix 1 to Mix 2.

Artificial flaws were used in this study to recover the tensile ductility of Mix 2. Introduction of artificial flaws has been demonstrated to effectively enhance the multiple cracking behavior and improve the ductility of ECC mixes in a previous study [38]. In this study, 3% (by volume fraction) of polystyrene beads (Fig. 9) of 4 mm size were added to the mix after adding the fiber. The uniaxial tensile test result of this modified mix is shown in Fig. 10. The first crack strength drops slightly from 1.58 MPa to 1.53 MPa on average compared to Mix 2, which indicates that the natural pre-existing flaws in Mix 2 are slightly smaller than the beads. By adding the artificial flaws, a larger margin between σ_0 and σ_{cs} has been achieved. The relatively large flaws of similar size initiate a large number of cracks at small stress interval and result in an average strain capacity of 2.15%. Fig. 11 shows the crack pattern

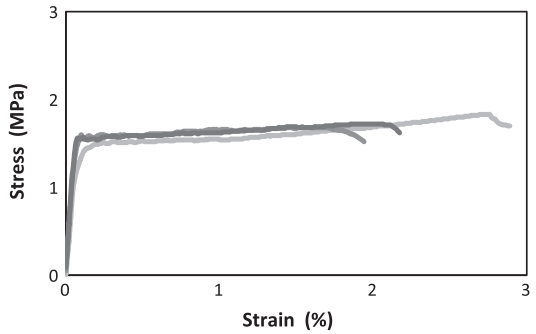

Fig. 10. Recovery of tensile ductility of Mix 2 by the addition of artificial flaws.

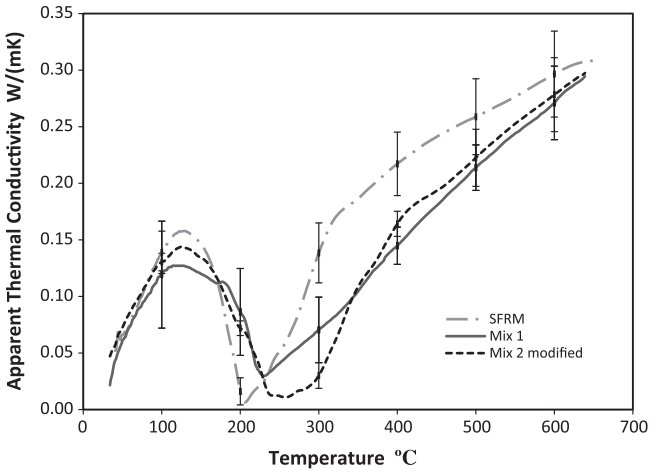

Fig. 12. Modified Mix 2 retains similar apparent thermal conductivity of unmodified FR-ECC (Mix 1).

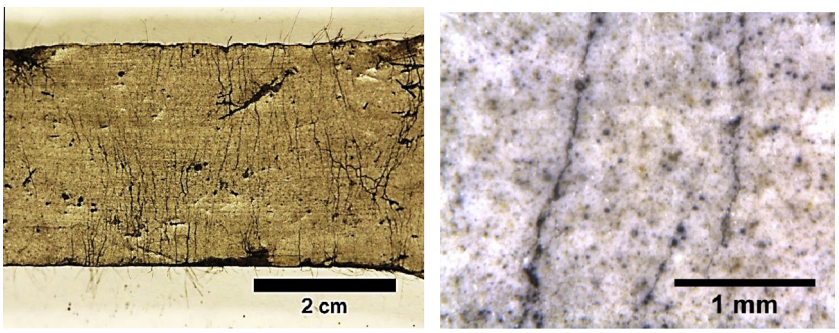

Fig. 11. Crack pattern of Mix 2 modified with artificial flaws.

of the modified specimens. In these pictures, carbon black solution was applied to the specimen surface after the tensile test to improve the visibility of the cracks. The left figure depicts the saturated multiple fine cracks throughout the specimen length. The right figure shows typical micro-cracks under optical microscope. The crack spacing is as narrow as 1 mm and the residual crack width is no more than 5 μm. The desired tensile ductility is restored in Mix 2 adjusted with 3% volume fraction of polystyrene beads serving as artificial flaws.

Experiments were also conducted to confirm that other targeted properties of Mix 2 are not altered by the addition of artificial flaws. The compressive strength of the new mixture (modified Mix 2) was measured to be 8.00 ± 0.34 MPa with a dry density of 575 kg/m^3. The adhesion (G_c) for the modified FR-ECC (with full 2% fiber content) was measured to be 70.0 ± 20.6 J/m^2 that is quite close to the unmodified Mix 2 (with G_c of 69.6 ± 36.9 J/m^2) with similar failure mechanism. Finally, the measured thermal conductivity (as detailed in Ref. [3]) of modified Mix 2 does not show significant difference from the original mix (Mix 1) as shown in Fig. 12. Therefore, the inclusion of polystyrene beads does not noticeably alter the other target properties.

4. Conclusions

The following conclusions can be drawn based on the experimental findings:

1. The apparent interfacial fracture energy of FR-ECC (matrix)/steel is measured to be 3 times higher than a conventional medium-density SFRM/steel, which tends to fail cohesively inside the SFRM near the interface. With significant increase in cohesive property of FR-ECC compared to SFRM, the failure mode was transformed to adhesive failure.
2. The hypothesis that latex bonding agent can enhance the FR-ECC/steel adhesive bond is experimentally confirmed. Latex bonding agent as admixtures is found to effectively improve the interfacial adhesion energy between FR-ECC (matrix) and steel by 54%. Alternatively, directly applying the bonding agent on the steel surface results in a dramatic improvement of adhesion energy by 147%. The adhesive bond improvement was significant enough to drive the failure mode from dominantly adhesive failure back to cohesive failure in the FR-ECC.
3. The enhancement of interfacial adhesion with latex modification is attributed to a change in composition and microstructure of the ITZ between the FR-ECC (matrix) and steel, as confirmed by SEM with EDAX.
4. Latex polymer bonding agent as admixtures was found to reduce the tensile ductility and compressive strength of FR-ECC. Nevertheless, the compressive strength of 6.40 MPa is within the acceptable range for fire-resistive materials.
5. The use of artificial flaws was found to be effective in restoring the tensile ductility of FR-ECC containing latex. This modified FR-ECC possesses remarkably improved mechanical properties (with compressive strength of 8.00 MPa, tensile strength of 1.75 MPa and tensile ductility of 2.15%) over conventional SFRM, while maintaining similar thermal conductivity. The adhesion energy G_c for the modified FR-ECC/steel was found to be 70.0 ± 20.6 J/m^2, about 6.3 times that of SFRM/steel at 11.1 J/m^2.

Acknowledgments

The authors wish to express their gratitude and sincere appreciation to 3 M (glass bubbles), Lafarge (cement), WR Grace (SP and VMA), Dayton Superior (bonding agent) and Kuraray (PVA fiber) for material supply for this research project.

References

[1] Liu TC, McDonald JE. Prediction of tensile strain capacity of mass concrete. ACI J Proc 1978;75(5):192–7.
[2] Li VC. On engineered cementitious composites (ECC) – a review of the material and its applications. J Adv Concr Technol 2003;1(3):215–30.
[3] Zhang Q, Ranade R, Li VC. Feasibility study on fire-resistive engineered cementitious composites. ACI Mater J; 2014 [in press].
[4] Li G, Kodur V. Role of insulation effectiveness on fire resistance of steel structures under extreme loading events. J Perform Constr Facil 2011;25(4).
[5] ASTM E736-00: standard test method for cohesion/adhesion of sprayed fire-resistive materials applied to structural members. West Conshohocken (PA): ASTM International; 2011. doi: http://dx.doi.org/10.1520/E0736-00R11. <www.astm.org>.
[6] Tan KT, White CC, Hunston DL. An adhesion test method for spray-applied fire-resistive materials. Fire Mater 2011;35:245–59.
[7] Bentz DP, White CC, Prasad KR, Flynn DR, Hunston DL, Tan KT. A materials science-based approach to characterizing fire resistive materials. J ASTM Int 2009;6(5).
[8] Nakayama M, Beaudoin JJ. Bond strength development between latex-modified cement paste and steel. Cem Concr Res 1987;17(4):562–72.
[9] Najm H, Naaman AE, Chu T-J, Robertson RE. Effects of poly(vinyl alcohol) on fiber cement interfaces. Part I: Bond stress–slip response. Adv Cem Based Mater 1994;1(3):115–21.
[10] Gao JM, Qian CX, Wang B, Morino K. Experimental study on properties of polymer-modified cement mortars with silica fume. Cem Concr Res 2002;32(1):41–5.
[11] Fu X, Chung DDL. Improving the bond strength between steel rebar and concrete by ozone treatment of rebar and polymer addition to concrete. Cem Concr Res 1997;27(5):643–8.
[12] Chew MYL. Factors affecting ceramic tile adhesion for external cladding. Constr Build Mater 1999;13(5):293–6.
[13] Jenni A, Holzer L, Zurbriggen R, Herwegh M. Influence of polymers on microstructure and adhesive strength of cementitious tile adhesive mortars. Cem Concr Res 2005;35(1):35–50.
[14] Brien JV, Mahboub KC. Influence of polymer type on adhesion performance of a blended cement mortar. Int J Adhes Adhes 2013;43:7–13.
[15] Su Z. Microstructure of polymer cement concrete. Delft, The Netherlands: Delft University Press; 1995.
[16] Chandra S, Ohama Y. Polymers in concrete. Boca Raton, Fla.: CRC Press; 1994.
[17] Kim J, Robertson RE, Naaman AE. Structure and properties of poly(vinyl alcohol)-modified mortar and concrete. Cem Concr Res 1999;29(3):407–15.
[18] Ohama Y, Ota M. Recent trends in research and development activities of polymer-modified paste, mortar and concrete in Japan. Adv Mater Res 2013;687:26–34.
[19] Li VC, Wu C, Wang S, Ogawa A, Saito T. Interface tailoring for strain-hardening polyvinyl alcohol-engineered cementitious composites (PVA-ECC). ACI Mater J 2002;99(5):463–72.
[20] Kanda T, Li VC. A new micromechanics design theory for pseudo strain hardening cementitious composite. ASCE J Eng Mech 1999;125(4):373–81.
[21] Li VC. Engineered cementitious composites – tailored composites through micromechanical modeling. In: Banthia N, Bentur A, Mufti A, editors. Fiber reinforced concrete: present and the future. Canadian Society for Civil Engineering, Montreal, Quebec, Canada; 1998. p. 64–97.
[22] Ohama Y. Handbook of polymer-modified concrete and mortars: properties and process technology. William Andrew; 1995.
[23] Ramakrishnan V. Properties and applications of latex-modified concrete. In: Malhotraed VM, editor. Advances in concrete technology. 2nd ed. Canada Centre for Mineral and Energy Technology; 1994. p. 839–90.
[24] Ohama Y. Polymer-based admixtures. Cem Concr Compos 1998;20(2):189–212.
[25] Rossignolo João A, Agnesini Marcos VC. Mechanical properties of polymer-modified lightweight aggregate concrete. Cem Concr Res 2002;32(3):329–34.
[26] Song SH, Liu FT. Influences of polymer fiber and polymer latex on physical properties of cement mortar. Adv Mater Res 2011;306:814–8.
[27] ASTM Standard C109: standard test method for compressive strength of hydraulic cement mortars (using 2-in. or [50-mm] cube specimens). Philadelphia, PA; 2002.
[28] JSCE: recommendations for design and construction of high. Performance fiber reinforced cement composites with multiple fine cracks (HPFRCC), March; 2008.
[29] Mindess S, Young F, Darwin D. Concrete. 2nd ed.; 2003.
[30] Struble L. Microstructure and fracture at the cement paste–aggregate interface. In: Proceedings of symposium on bonding in cementitious composites, vol. 114. Materials Research Society, Pittsburgh; 1988. p. 11–20.
[31] Mansur AAP, Santos DB, Mansur HS. A microstructural approach to adherence mechanism of poly (vinyl alcohol) modified cement systems to ceramic tiles. Cem Concr Res 2007;37(2):270–82.
[32] Kim J, Robertson RE. Effect of polyvinyl alcohol on aggregate–paste bond strength and the interfacial transition zone. Adv Cem Based Mater 1998;8(2):66–76.

[33] Mindess S. "How important is it" bonding in cementitious composites. Materials Research Society, Pittsburgh; 1988. p. 3–10.
[34] Su Z, Bijen JM, Larbi JA. Influence of polymer modification on the hydration of Portland cement. Cem Concr Res 1991;21(2–3):242–50.
[35] Zhang X, Groves GW, Rodger SA. The microstructure of cement aggregate interfaces. In: Bonding in cementitious composites. Materials Research Society, Pittsburgh; 1988. p. 89–95.
[36] UFGS-07 81 00: spray-applied fireproofing, February; 2011.
[37] ICC-ES, AC23: acceptance criteria for spray-applied and intumescent mastic coating fire-protection materials; 2011.
[38] Wang S, Li VC. Tailoring of pre-existing flaws in ECC matrix for saturated strain hardening. In: Proceedings of FRAMCOS-5, Vail, Colorado, USA; 2004. p. 1005–12.